IEICE Proceeding Series

Synchronizability and dynamics of coupled neural mass oscillators

Daniel Malagarriga, Jordi Garcia-Ojalvo, Antonio J. Pons

Vol. 1 pp. 493-496
Publication Date: 2014/03/17
Online ISSN: 2188-5079

2012 International Symposium on Nonlinear Theory and its Applications
NOLTA2012, Palma, Majorca, Spain, October 22-26, 2012

Synchronizability and dynamics of coupled neural mass oscillators

Daniel Malagarriga, Jordi Garcia-Ojalvo and Antonio J. Pons

Departament de Fisica i Enginyeria Nuclear, Universitat Politecnica de Catalunya
Edif. Gaia, Rambla Sant Nebridi s/n, 08222 Terrassa, Spain
Email: daniel.malagarriga@upc.edu, jordi.g.ojalvo@upc.edu, a.pons@upc.edu

Abstract—We study the collective behavior of a system of coupled neural mass oscillators that represent the voxels of a cortical area of the brain. Each neural mass model, which describes three populations of cortical neurons linked to each other via excitatory and inhibitory connections, receives a periodic driving from subcortical structures that relay sensory inputs. We examine how the dynamics and synchronizability of the represented cortical voxels change with the inter-voxel coupling strength, for both excitatory and inhibitory coupling. Our results show that an intermediate level of excitatory coupling leads to a regime in which the dynamics is both irregular and synchronized among voxels. The results obtained shed light on how brain dynamics depends on coupling within cortical areas.

1. Introduction

Synchronization appears in many different systems formed by coupled dynamical units. This phenomenon, which has been intensely studied in the last couple of decades [1], is often analyzed using toy models that have simple dynamics (e.g. periodic oscillations) [2]. In other cases, synchronization appears in systems that display complex dynamical behavior. It has been shown, for instance, that coupled chaotic units may synchronize in some cases [3]. A relevant example of a system that shows extremely complex dynamics but requires an optimal amount of synchrony for its normal function is the brain. An excess of brain synchronization in certain locations of the brain may lead, for instance, to epilepsy or Parkinson's disease [4]. Insufficient synchronization in certain frequency bands, on the other hand, may cause other problems such as Alzheimer's disease and autism [5]. Besides, the coordinated activity in the brain operates at different spatial and time scales. For instance, ensembles of neurons organize their (microscopic) spiking activity via synchronization [6]. The result of this synchronized activity is an oscillatory behavior of the average activity of the neuronal ensemble [7]. This average activity of mesoscopic populations of neurons becomes the dynamical observable of the neural mass model used in this work. At a larger, more macroscopic scale, the activity (measured with non-invasive techniques such as fMRI, EEG and MEG) of different brain areas that participate in a specific task also indicate, in some cases, a high degree of synchronization.

In this paper, we study the synchronizability and irregularity of the dynamics of neural populations at the mesoscopic scale. To do so, we will consider as our dynamical system a set of coupled neural mass models, namely voxels, which describe cortical columns composed by three populations of neurons linked to each other via excitatory and inhibitory connections. Each cortical column receives a periodic driving from a subcortical structure, e.g., the thalamus. Our aim is to analyze the synchronizability and regularity of this system's dynamics, in terms of the excitatory and inhibitory inter-voxel coupling.

2. The model

We use an extended version of the model introduced by Jansen and coauthors [8, 9]. Jansen's model describes the dynamics of a cortical column. The neurons in this cortical column are grouped in three different populations: pyramidal, excitatory interneurons and inhibitory interneurons. Their coupling architecture is organized as follows. The pyramidal population excites the excitatory and inhibitory interneuron populations in a feedforward manner, and receives in turn inhibitory and excitatory feedback from them. The pyramidal population receives an incoming pulse density $p(t)$ that includes excitatory, $p_e(t)$, and inhibitory, $p_i(t)$, inputs from neighboring cortical columns, and a periodic driving coming from the thalamus, $p_T(t)$. The three populations transform the total average density of action potentials arriving to their synapses from different origins, $\sum_m p_m(t)$, into an average postsynaptic membrane potential, $y_i(t)$, which can be either excitatory or inhibitory. The integration of the total average density of action potentials, $\sum_m p_m(t)$, performed at the (excitatory) synapses of the populations is implemented by the differential operator $L(y_i(t); a)$ defined in the following way:

$$L(y_i(t);a) = \frac{d^2 y_i(t)}{dt^2} + 2a\frac{dy_i(t)}{dt} + a^2 y_i(t) = Aa\left[\sum_m p_m(t)\right] \quad (1)$$

and similarly for the inhibitory coupling, $L(y_i(t); b)$.

The transformation of the total average postsynaptic potential of each population, $m(t) = y_{exc}(t) - y_{inh}(t)$, into an average density of action potentials, $p_m(t) = \lambda S(m(t))$, takes place in the somas and is described by a sigmoidal function:

$$S(m(t)) = \frac{2e_0}{1 + e^{r(\nu_0 - m(t))}} \quad (2)$$

weighted by the coupling constant, λ. e_0 determines the maximum firing rate of the neural population, ν_0 is the PSP for which a 50% firing rate is achieved and r the steepness of the sigmoidal transformation. Four connectivity constants (C_p with $p = 1, ..., 4$) represent the coupling intensity between the three populations which form each cortical column.

We consider a set of n cortical columns, voxels, arranged in an all-to-all connectivity configuration. The full model for each cortical column i (with $i = 1, \ldots, n$) connected to other cortical columns j (with $j \neq i$, $j = 1, \ldots, n$), is:

$$L(y_0^i(t); a) = Aa\{S(y_1^i(t) - y_2^i(t))\} \quad (3)$$

$$L(y_1^i(t); a) = Aa\{C_2 S(C_1 y_0^i(t)) + \bar{p}^i + \delta \sin(2\pi f t) + \alpha \sum_{\substack{j=1 \\ j\neq i}}^{n} \frac{1}{n-1} S(y_1^j(t) - y_2^j(t))\} \quad (4)$$

$$L(y_2^i(t); b) = Bb\{S(y_1^i(t) - y_2^i(t)) + \beta \sum_{\substack{j=1 \\ j\neq i}}^{n} \frac{1}{n-1} S(y_1^j(t) - y_2^j(t))\} \quad (5)$$

where $y_0(t)$, $y_1(t)$ and $y_2(t)$ correspond to the excitatory postsynaptic potential input to the interneuron population, the excitatory postsynaptic potential input to the pyramidal population and the inhibitory postsynaptic potential input to the pyramidal population, respectively. The parameter values of the model are the same as those of Jansen et al. [8] except for $C = 133.5$ (see the relation of this parameter with C_p in ref. [8]). These equations have been solved numerically using the Heun method [10].

3. Results

3.1. Isolated voxel

Even though single cortical columns modeled by Jansen's model show regular behavior when $\bar{p}$ is maintained constant [11, 12], they display complex behavior when driven periodically [13, 14]. In Fig. 1a, we show a time trace of $(y_1(t) - y_2(t))$ obtained for a cortical column with a constant driving $\bar{p} = 155.0$ with and without thalamic periodic driving. In Fig. 1b, we show the power spectra of the corresponding signals. This figure shows that those cortical columns which do not receive a (significative) driving from subcortical structures behave periodically, with a peak centered around 11 Hz, in the range of the upper alpha band. However, those cortical columns which do receive a (significative) thalamic driving, which oscillates at around 8 Hz (in the lower alpha band), may show chaotic behavior. In this case, the power spectrum does not exhibit a single narrow peak, but takes the form of a wide band with a dominant peak centered at the thalamic driving frequency. Ponten et al. [15] have shown that the dynamical behavior of a set of coupled neural mass oscillators forming a network with irregular architecture is organized (is phase coherent) at the functional level. These two results, say, the (ir)regularity promoted by the thalamic driving and the synchronizability appearing in the activity of the cortical area enhanced by the column-column coupling may vary considerably when the intensity and the na-

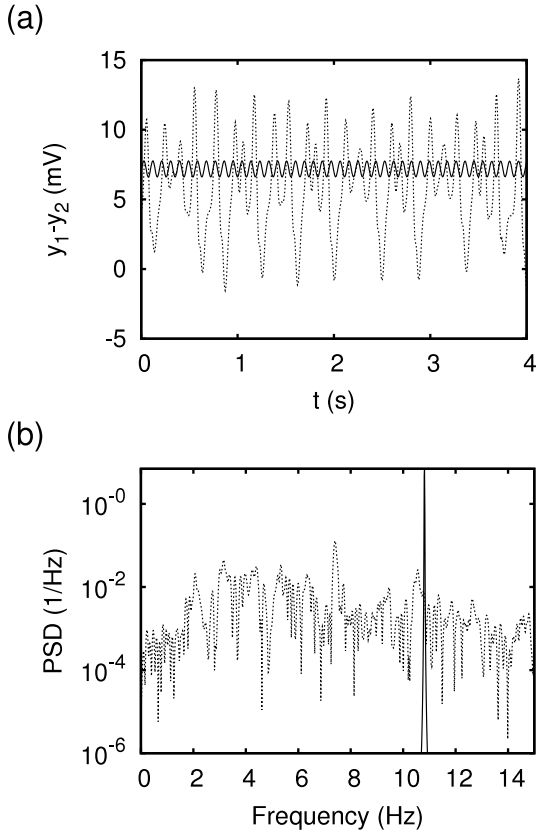

Figure 1: Dynamics of an isolated cortical column. Both regular and irregular dynamics are obtained with Jansen's model depending of the driving conditions. (a) Time trace of $(y_1(t) - y_2(t))$ for a system with (dashed line) and without (solid line) thalamic driving. (b) Power spectrum of the data shown in (a). $\bar{p} = 155.0$ and $\delta = 0$ (solid line), $\delta = 64$, $f = 7.4$ (dashed line).

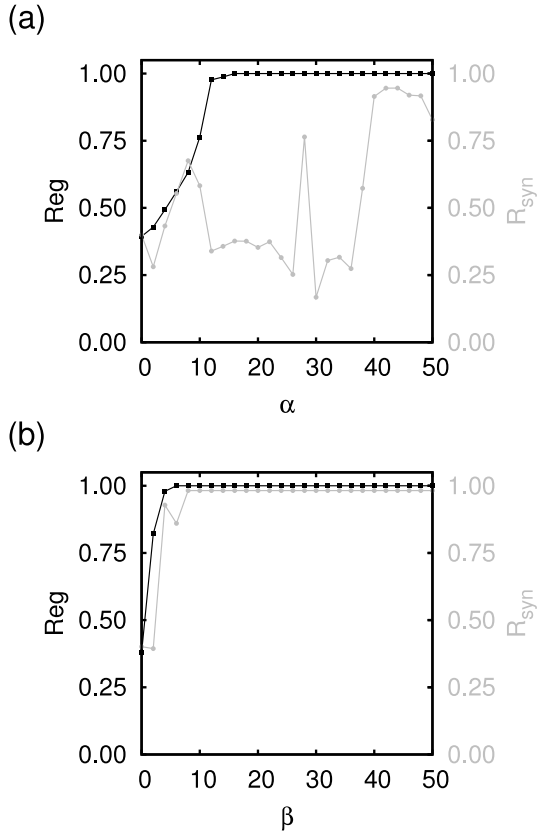

Figure 2: Regularity, *Reg* (black), and synchronization, R_{syn} (gray) parameters in terms of the coupling intensities for an ensemble of $n = 50$ periodically driven cortical columns. (a) Results obtained when increasing the excitatory coupling intensity, α. (b) Results obtained when increasing the inhibitory coupling intensity, β.

ture of the coupling (excitatory and inhibitory) are changed. Somehow, a competition between the irregular dynamical behavior appearing when the thalamic driving dominates the input and the synchronizability with neighboring cortical columns enhanced by the neighboring column cortical coupling is established.

3.2. Cortical area dynamics

In order to model the activity of a cortical area, we have considered a system of $n = 50$ coupled cortical columns modeled by Eqs. (3)-(5) for varying coupling parameters α and β, and a constant thalamic driving with $\delta = 64$ and $f = 7.4$. These parameter values have been chosen because they lead to a broad power spectrum (i.e. the dynamics is irregular). We have analyzed the variation of regularity and synchronization when changing the coupling parameters. Specifically, we have performed $s = 100$ realizations of the dynamics at each value of α or β. To quantify how the dynamics is, we define a regularity parameter, Reg, as the average of the height of the second peak $h_2(\tau)$ of the autocorrelation function of $m^i(t) = y_1^i(t) - y_2^i(t)$:

$$\mathrm{Reg} = \frac{1}{s}\frac{1}{n}\sum_{t=1}^{s}\sum_{q=1}^{n} h_2(\tau), \qquad (6)$$

where the sums run over the s realizations and n cortical columns. In order to quantify the synchronization, we define a synchronization parameter R_{syn} as the average of the maximum of the cross-correlation function, $C(\tau)$, of $m^i(t)$ between pairs of cortical columns:

$$R_{syn} = \frac{1}{s}\frac{1}{n(n-1)}\sum_{t=1}^{s}\sum_{\substack{p=1\\p\neq q}}^{n} \max(|C(\tau)|). \qquad (7)$$

Figure 2 shows these two parameters, Reg and R_{syn}, for increasing values of α and β. Figure 2a reveals, in particular, that even though synchronization increases very quickly when the excitatory coupling between cortical columns increases, regularity is maintained very low for intermediate values of α (here $\beta = 0$). This behavior is not observed when the coupling is inhibitory (see Fig. 2b): inhibitory coupling (with $\alpha = 0$) seems to increase the regularity of the dynamics and the synchronization of the cortical columns at the same rate. The efficiency of the inhibitory coupling to increase both parameters is larger than that shown when increasing excitatory coupling.

4. Conclusions

We have considered a model which mimics the activity of an ensemble of cortical columns that represent a small cortical area driven by a subcortical structure such as the thalamus. These cortical colums are connected in an all-to-all configuration. The irregular dynamics obtained for a driven single column and the synchronizability of the system have been studied when increasing the excitatory and inhibitory coupling within the area. Our results show that both the regularity and the synchronizability depend strongly on the nature of the coupling. On the one hand, excitatory coupling allows to synchronize the whole area maintaining, for a wide range of intensities, the irregular nature of the cortical activity. On the other hand, inhibitory coupling is much more effective destroying the irregular activity allowing for a stronger synchronization even for small coupling intensities. The ability of the excitatory connections to synchronize neuronal populations while maintaing a complex dynamics makes possible larger integration capabilities, specially when considering the interaction of different cortical areas working at the macroscopic level.

Acknowledgements

This research was partially supported by MICINN (Spain) under project FIS2009-13360 and by the Generalitat de Catalunya (project 2009-SGR-1168). D.M. is funded by a FPU-UPC PhD fellowship. J.G.O. also acknowledges support by the ICREA Academia Programme.

References

[1] A. Pikovsky, M. Rosenblum, and J. Kurths. *Synchronization: A universal concept in nonlinear sciences*. 12. Cambridge University press, 2001.

[2] Steven H Strogatz. From Kuramoto to Crawford: exploring the onset of synchronization in populations of coupled oscillators. *Physica D*, 143:1–20, 2000.

[3] S. Boccaletti, J. Kurths, G. Osipov, D.L. Valladares, and C.S. Zhou. The synchronization of chaotic systems. *Physics Reports*, 366(1-2):1–101, August 2002.

[4] Alfons Schnitzler and Joachim Gross. Normal and Pathological oscillatory communication in the brain. *Nature Reviews Neuroscience*, 6(April):285–296, 2005.

[5] Peter J Uhlhaas and Wolf Singer. Neural Synchrony in Brain Disorders: Relevance for Cognitive Dysfunctions and Pathophysiology. *Neuron*, 52:155–168, 2006.

[6] D Hansel, G Mato, and C Meunier. Synchrony in excitatory neural networks. *Neural Comput*, 7(2):307–37, Mar 1995.

[7] György Buzsáki and Andreas Draguhn. Neuronal oscillations in cortical networks. *Science*, 304(5679):1926–9, Jun 2004.

[8] B H Jansen and V G Rit. Electroencephalogram and visual evoked potential generation in a mathematical model of coupled cortical columns. *Biol Cybern*, 73(4):357–66, 1995.

[9] B. H. Jansen, G. Zouridakis, and M. E. Brandt. A neurophysiologically-based mathematical model of flash visual evoked potentials. *Biol. Cybern.*, 68:275–283, 1993.

[10] J. Garcia-Ojalvo and J. M. Sancho. *Noise in spatially extended systems*. Springer Verlag, 1999.

[11] François Grimbert and Olivier Faugeras. Bifurcation analysis of Jansen's neural mass model. *Neural Computation*, 18(12):3052–68, 2006.

[12] Andreas Spiegler, Stefan J. Kiebel, Fatihcan M. Atay, and Thomas R. Knösche. Bifurcation analysis of neural mass models: Impact of extrinsic inputs and dendritic time constants. *NeuroImage*, 52(3):1041 – 1058, 2010.

[13] Andreas Spiegler, Thomas R. Knösche, Karin Schwab, Jens Haueisen, and Fatihcan M. Atay. Modeling brain resonance phenomena using a neural mass model. *PLoS Comput Biol*, 7(12):e1002298, 12 2011.

[14] Gan Huang, Dingguo Zhang, Jiangjun Meng, and Xiangyang Zhu. Interactions between two neural populations: A mechanism of chaos and oscillation in neural mass model. *Neurocomputing*, 74(6):1026 – 1034, 2011.

[15] S.C. Ponten, A. Daffertshofer, A. Hillebrand, and C.J. Stam. The relationship between structural and functional connectivity: Graph theoretical analysis of an eeg neural mass model. *NeuroImage*, 52(3):985 – 994, 2010.